Fabrication of Gold Nanodot Array on Plastic Films for Bio-sensing Applications

Article · December 2013

DOI: 10.1016/j.procir.2013.01.009

4 authors, including:

Phuc T. D.
Tokyo Institute of Technology
8 PUBLICATIONS **22** CITATIONS

SEE PROFILE

Masahiko Yoshino
Tokyo Institute of Technology
168 PUBLICATIONS **947** CITATIONS

SEE PROFILE

Akinori Yamanaka
Tokyo University of Agriculture and Technology
183 PUBLICATIONS **1,016** CITATIONS

SEE PROFILE

Available online at www.sciencedirect.com

SciVerse ScienceDirect

Procedia CIRP 5 (2013) 47 – 52

www.elsevier.com/locate/procedia

The First CIRP Conference on Biomanufacturing

Fabrication of gold nanodot array on plastic films for bio-sensing applications

Truong Duc Phuc[a,*], Masahiko Yoshino[a], Akinori Yamanaka[b], Takatoki Yamamoto[a]

[a]*Department of Mechanical and Control Engineering, Tokyo Institute of Technology, 2-12-1 Ookayama, Meguro-ku, Tokyo 152-8550, Japan*

[b]*Department of Mechanical Systems Engineering, Tokyo University of Agriculture and Technology, 2-24-16 Nakacho, Koganei-shi, Tokyo, 184-8588, Japan*

* Corresponding author. Tel.: +81-3-5734-2640; fax: +81-3-5734-2640. *E-mail address*: phuc.t.aa@m.titech.ac.jp

Abstract

In this paper, authors propose a new method to fabricate metal nanodot array on a plastic film. This process comprises three steps; firstly, a substrate is deposited with metal. Then, a nanodot array is formed on the substrate surface by thermal dewetting. Finally, the nanodot array is transferred to a plastic film. Using the proposed method, gold nanodot array is fabricated on epoxy films. Furthermore, in this paper, the effects of process parameters such as annealing temperature, substrate material and plastic material on dot transfer ratio to a plastic film are studied. The mechanism of dot transfer from a substrate to a plastic film is also discussed in details. The transfer ratio increases as the annealing temperature is higher. Silicon substrate results slightly higher contact angle and transfer ratio than quartz glass substrate. Araldite rapid epoxy decreases transfer ratio while SpeciFix-20 epoxy increases transfer ratio when the annealing temperature is higher. Highest transfer ratios of 95% and 87% were achieved when transferring nanodot array from silicon substrate and quartz glass substrate to Araldite rapid epoxy film, respectively. Highest transfer ratio of 91% was achieved when transferring nanodot array from quartz glass substrate to SpeciFix-20 epoxy.

Selection and/or peer-review under responsibility of Professor Mamoru Mitsuishi and Professor Paulo Bartolo

Keywords: Gold Nanodot Array; Thermal Dewetting; Nanodot Transfer; Plastic Film

1. Introduction

Recently, metallic nanodot arrays have been attracting interest because of their unique optical property such as localize surface plasmon resonance (LSPR), LSPR is a collective oscillation of the conduction electrons on the surface of nanodots when they are excited by incident light of specific wavelengths. Large electromagnetic field enhancement at the LSPR frequency [1, 2] on the surface of metallic nanodot induces very strong absorption and scattering of the light. This makes metallic nanodots very auspicious to be applied to dark field imaging [3-6], bio-sensing [5-9], photo-thermal therapy [10-12] and plasmonic solar cells [2, 13-16], etc. A nanodot array is regularly aligned nanodots. It is known that the LSPR property depends on the shape, size, arrangement of the nanodot and dielectric constant of medium surrounding the nanodot [5, 10, 11, 17, 18]. For this reason, adding bio species such as proteins, anti-bodies, etc. on the surface of nanodot array causes the shift of LSPR peak. Change of bio species on nanodot array can be detected by variation of LSPR peak. Furthermore, the shape, size and arrangement of nanodot array can be tuned to enhance plasmonic sensitivity. Therefore, nanodot arrays

2212-8271
Selection and/or peer-review under responsibility of Professor Mamoru Mitsuishi and Professor Paulo Bartolo
doi:10.1016/j.procir.2013.01.009

can be applied to high sensitivity bio sensing devices.

Usually, nanodot arrays can be fabricated by conventional top-down nanofabrication methods like EB lithography or UV lithography [19, 20]. The advantage of these methods is high accuracy fabrication (shape, size, arrangement of the nanodot array). However, these methods are very stringent, complicated and low throughput. Also, the production cost is high due to expensive equipment. On the other hand, bottom-up methods such as self-assembly method [21, 22] is suitable to fabricate nanodots of some tens nanometer in diameter at a very high throughput. However, the uniformity and regularity of the nanodot array fabricated by bottom-up methods are low. In order to obtain ordered nanodot arrays, the authors developed a combined process of metal deposition, patterning by nano plastic forming (NPF) and annealing [23]. However, only substrates of high melting temperature materials such as silicon, quartz, etc. are available in this process. The new idea in this study is to make ordered nanodot arrays on plastic films which can be flexibly utilized in more variety of applications. Moreover, plastic (polymer) substrate is more useful for bio devices, because it is flexible, light weight, low cost, durable, chemical resistant and reliable, etc. Fabrication of metallic nanodot array on plastic substrates will broaden its applications and considerably reduces the production cost.

The objective of this research is to develop a new process to fabricate a metal nanodot array on a plastic film by combination of metal deposition, thermal dewetting and transferring nanodot array to a plastic film, and to study the effect of process parameters on dot transfer ratio to a plastic film. In this paper, the effect of annealing temperature, substrate material and plastic material on the transfer ratio of random nanodot array to a plastic film is studied.

2. Experiment method

Figure 1 shows the proposed process to fabricate nanodot array on a plastic film. The process comprises three steps; firstly, substrate is deposited with metal. Then, the nanodot array is formed on the substrate surface by thermal dewetting. Finally, the nanodot array is transferred to a plastic film. The experiments were conducted as follows:

Silicon <110> substrate and quartz glass substrates of 10 mm × 10 mm × 1 mm in size were used for the experiment. The substrates were cleaned by ultrasonic vibration in an acetone bath for 10 minutes. After the substrates were dried, gold was deposited on the surface of the substrates by a DC sputter coater. The sputter gas was argon, and its pressure was 0.1 MPa. The distance between the substrate and a gold target was 35 mm. The sputtering current was kept to 5 mA during sputter deposition. The thickness of the deposited gold layer was controlled to 8 nm by controlling the sputtering time. The gold coated substrates were annealed in an electrical furnace for 10 minutes at various temperatures; 600°C, 700°C, 800°C, 900°C and 1000°C. Then, the specimens were taken out of the furnace and cooled down in air atmosphere. The nanodots on silicon substrate and quartz glass substrates were then observed by a field-emission scanning electron microscope (FE-SEM). Each substrate was dried by blowing hot air by a drier for 2 minutes to improve the adhesion between nanodots and plastic film. Then, the substrates were coated with a thin layer of epoxy mixtures. Two kinds of epoxy were tested in the experiments; one is Araldite rapid epoxy (a high viscosity epoxy) and the other is SpeciFix-20 epoxy (a low viscosity epoxy). The processing conditions for each epoxy are as follows:

Araldite rapid epoxy mixture (mass ratio of epoxy:curing agent is 1:1) was coated on the nanodots surface. Then, the epoxy coated substrate was cured at room temperature for 48 hours to completely harden the epoxy film. Finally, the epoxy film was peeled off from the substrate.

SpeciFix-20 epoxy mixture (mass ratio of epoxy:curing agent is 7:1) was coated on the nanodots surface. The epoxy coated substrate was put in vacuum chamber for 15 minutes to remove the bubbles and gas at the interface between the nanodots and the epoxy. Then, the epoxy was cured at room temperature for 48 hours. Finally, the epoxy film was peeled off from the substrate.

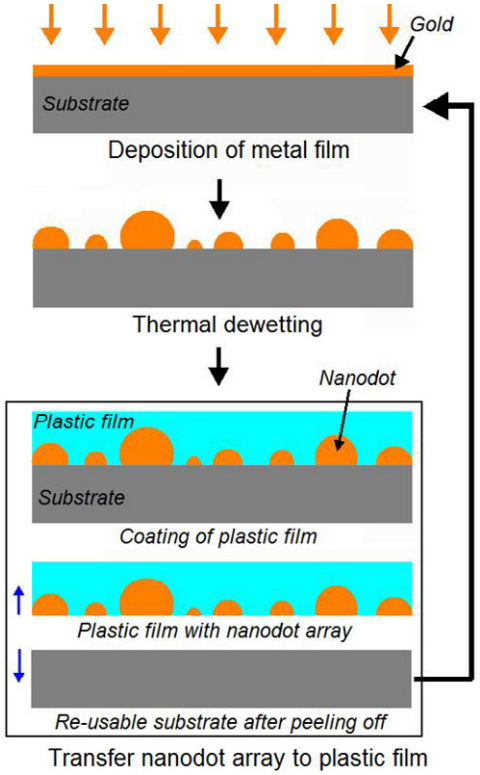

Fig. 1. Schematic schedule of process to fabricate nanodot array on plastic film

Nanodot arrays formed on the quartz glass substrate and the silicon substrate before transferring and nanodot array on the epoxy films after transferring were observed by a FE-SEM. Five points were observed for each specimen. Each experiment condition is repeated three times. The number of dots, mean diameter and contact angle of nanodots were calculated by using a graphic analysis system (ImageJ software). Transfer ratio was calculated as the ratio of the number of dots on the plastic film against that on the substrate.

3. Result and discussion

3.1. Effects of substrate material, plastic material and annealing temperature on dot transfer ratio

Figure 2 shows the FE-SEM micrographs of gold nanodots aggregated on (a) quartz glass substrate and (b) silicon substrate, after annealing at different annealing temperatures. It is observed that many gold dots smaller than 100nm were fabricated by annealing. It seems that the dots are smaller when the annealing temperature is higher. Also, it is found that the dots shape becomes more circular when the annealing temperature becomes higher.

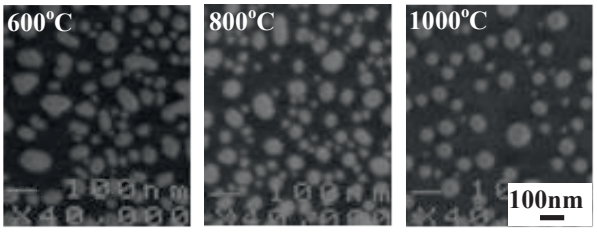

(a) Quartz glass substrate

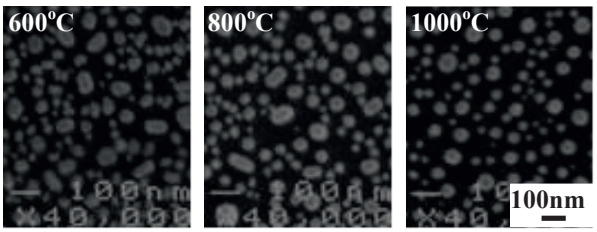

(b) Silicon substrate

Fig. 2. FE-SEM micrographs of gold nanodot formed on (a) quartz glass substrate and (b) silicon substrates after annealing at different temperatures

Figure 3 shows the variation of the mean diameter and its standard deviation of the nanodots against annealing temperature. It is found from the figure that the mean diameter of the nanodots slightly decreases with the increase of the annealing temperature for both the quartz glass substrate and the silicon substrate. The mean diameter of nanodot array on the silicon substrate is smaller than that on the quartz glass substrate. The standard deviation also decreases when the annealing temperature becomes higher.

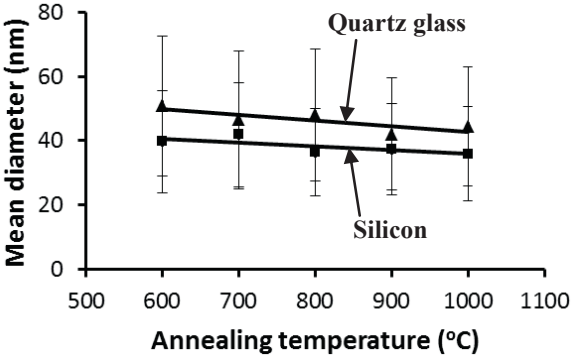

Fig. 3. Mean diameter and its standard deviation of gold nanodots versus annealing temperature

Figure 4 shows the variation of evaluated contact angle (see Appendix) of the nanodot array against annealing temperatures. It is found that the contact angle increases when the annealing temperature becomes higher. This is because the dots are not aggregated completely when the annealing temperature is low (from 600°C to 800°C). As seen in the Fig. 2, many distorted dots were generated at annealing temperatures lower than 800°C. Thus, the dots were still flat, and average contact angle was low. On the other hand, the dots were aggregated completely and were shaped in circular when the contact angle was high at higher annealing temperatures (900°C and 1000°C). Contact angle of the nanodot array on a silicon substrate is slightly higher than that of the nanodot array on a quartz glass substrate. This is because the surface energy of silicon <110> substrate is lower than that of quartz glass substrate (the surface energy of the silicon <110> substrate is 1510 erg/cm^2 [24] and that of the quartz glass substrate is 1825 erg/cm^2 [25]). According to Young's equation, the contact angle of the dot is higher when the surface energy of the substrate is lower.

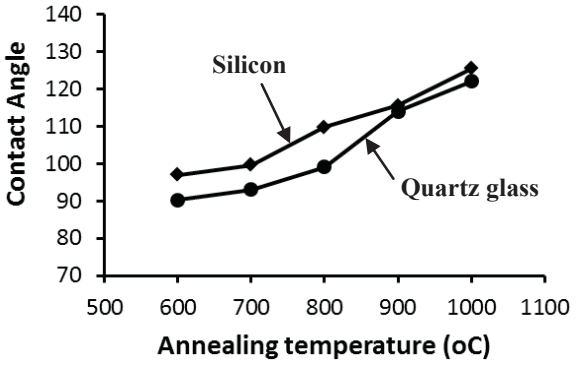

Fig. 4. Contact angle of nanodot array versus annealing temperature

Figure 5 shows the FE-SEM micrographs of the gold nanodot transferred to Araldite rapid epoxy films

from (a) quartz glass substrate and (b) silicon substrate. It is found that the gold nanodots were partly transferred to the epoxy films for all annealing temperatures from 600°C to 1000°C. Also, it seems that more dots were transferred to the epoxy films when the annealing temperature is lower.

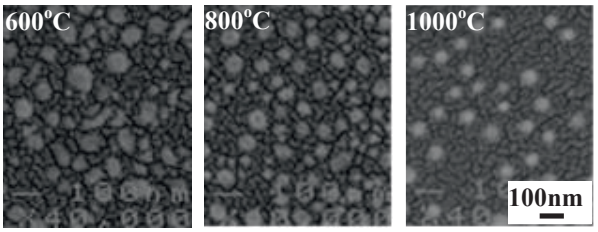

(a) Nanodots from quartz glass substrate transferred to Araldite rapid epoxy film

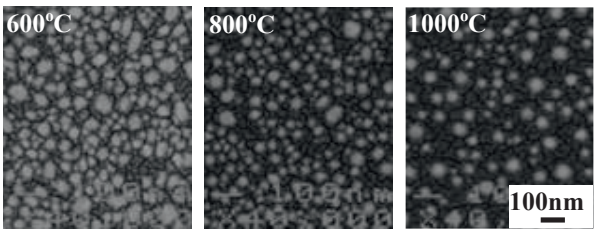

(b) Nanodots from silicon substrate transferred to Araldite rapid epoxy film

Fig. 5. FE-SEM micrographs of gold nanodots on Araldite rapid epoxy film transferred from (a) quartz glass substrate; (b) silicon substrate

Figure 6 shows the variation of the transfer ratio against annealing temperature. It is found that the transfer ratio decreases with the increase of annealing temperature for both the quartz glass substrate and the silicon substrate. The silicon substrate shows slightly higher transfer ratio than the quartz glass substrate. Highest transfer ratios of 95% and 87% were achieved for the silicon substrate and the quartz glass substrate, respectively, when annealing temperature is 600°C.

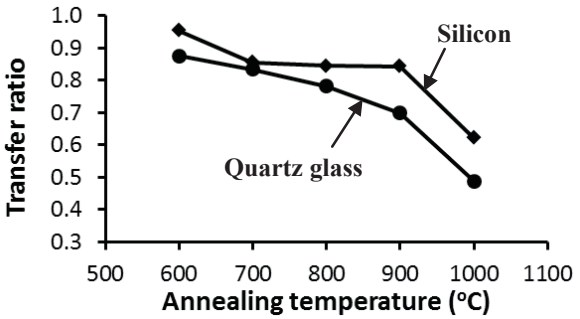

Fig. 6. Transfer ratio of gold nanodots versus annealing temperature

Figure 7 compares the variation of the transfer ratio of both plastic materials against annealing temperature. It is found that they show contrary trends in transfer ratio. The transfer ratio of the Araldite rapid epoxy decreases with the increase of annealing temperature while the SpeciFix-20 epoxy increases. Highest transfer ratios of 87% and 91% were achieved when transferring nanodot array from quartz glass substrate to Araldite rapid epoxy and SpeciFix-20 epoxy, respectively.

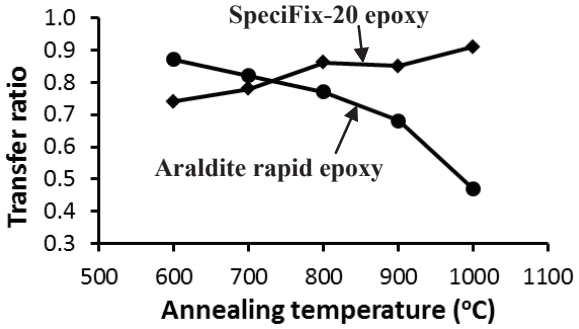

Fig. 7. Transfer ratio of Araldite rapid epoxy and SpeciFix-20 epoxy versus annealing temperature

3.2. Nanodot transfer mechanism

Effect of annealing temperature on the transfer ratio is explained by the total free energy of the dot/substrate/plastic film system. Fig. 8 shows a model of dot transfer operation; case I represents a dot remained on the substrate, and case II represents a dot transferred to the plastic film.

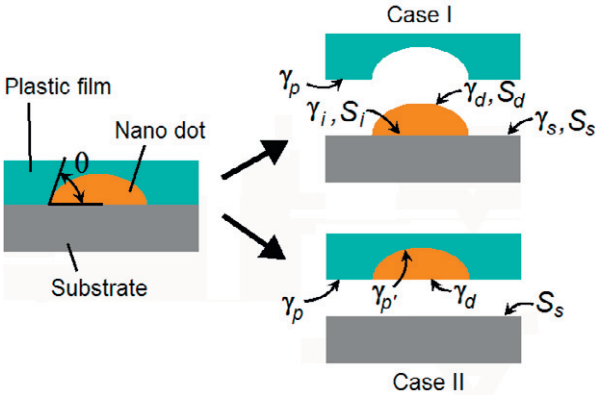

Fig. 8. Model of transferring nanodot from substrate to plastic film

If the dot is a sphere cap shape, the difference of the total free energy between case I and case II, ΔW, is calculated as in the following equation:

$$\Delta W = W_I - W_{II} = \begin{cases} \dfrac{\pi D^2}{4}\dfrac{\gamma_d}{1+\cos\theta}\left\{2\left(1+\dfrac{\gamma_p-\gamma_{p'}}{\gamma_d}\right)-(\cos\theta+1)^2\right\} & \theta < 90° \\ \dfrac{\pi D^2}{4}\gamma_d(1-\cos\theta)\left\{2\left(1+\dfrac{\gamma_p-\gamma_{p'}}{\gamma_d}\right)-(\cos\theta+1)^2\right\} & \theta \geq 90° \end{cases}$$

Where, W_I and W_{II} are total free energy of the system in case I and case II, respectively. D is the diameter of the

dot. γ_d and γ_p are the surface energy of the dot and the plastic film. γ_p, is the interfacial energy between the dot and the plastic film. θ is the contact angle between the dot and substrate. When $\Delta W > 0$, case II occurs, thus, the dot is transferred to the plastic film.

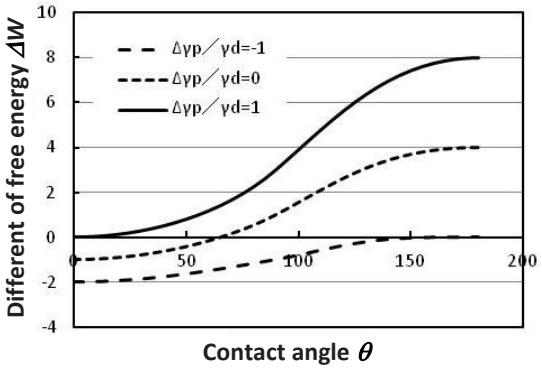

Fig. 9: Variation of ΔW against θ

Figure 9 shows the theoretical variation of ΔW against θ. It is found from the figure that ΔW increases with the increase of θ. This indicates that dot transfer becomes easier when θ becomes higher. The SpeciFix-20 epoxy agrees with the theoretical variation of transfer ratio which increases with the increase of contact angle. However, the Araldite rapid epoxy shows contrary variation of transfer ratio against contact angle. The reason is attributed to the difference between viscosities of the epoxies.

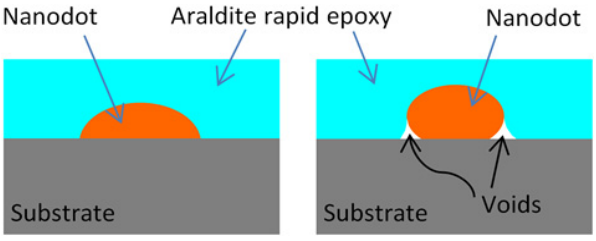

(a) Low contact angle (b) High contact angle

Fig. 10: Contact of high viscosity epoxy with the nanodot; (a) low contact angle; (b) high contact angle

The Araldite rapid epoxy is high viscosity resin and its flowability is poor. When the contact angle of the dot on the substrate is low, this resin is easier to be filled to the whole surface of the nanodot as shown in the Fig. 10 (a). However, when the contact angle of the dot on the substrate is higher, it is very difficult to fill the undercut at the bottom of the dot. Voids or air will exist at the undercut between the dot and the substrate as shown in the Fig. 10 (b). These voids reduce the contact area between the dot and the Araldite rapid epoxy film. It reduces the adhesion of the nanodots to the epoxy film. Therefore, even though the contact angle is higher at higher annealing temperature, the Araldite rapid epoxy results lower transfer ratios.

In contrast, the SpeciFix-20 epoxy is low viscosity resin and its flowability is good. It is believed that under vacuum atmosphere, low viscosity resin can be easily filled to the nanodot surface and obtained good contact with the nanodot and substrate as shown in the Fig. 11. The appearance of small bubbles on the surface of SpecFix-20 epoxy film inside the vacuum chamber may be attributed to the voids or air at the undercut between the nanodot and the quartz glass substrate. Under the vacuum atmosphere, these voids are filled with SpeciFix-20 epoxy and the air from the undercuts will float to the top of the epoxy film. As a result, higher contact angle increases contact area between nanodot and the epoxy film. Therefore, the transfer ratio increases with the increase of contact angle. This agrees with the theoretical variation as shown in the Fig. 9.

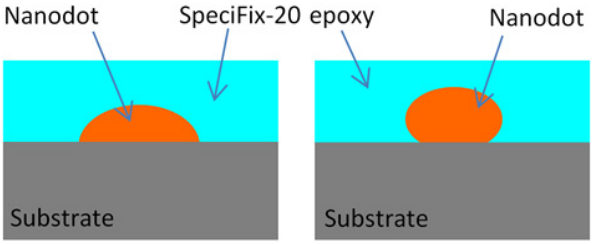

(a) Low contact angle (b) High contact angle

Fig. 11: Contact of low viscosity epoxy with the nanodot; (a) small contact angle; (b) high contact angle without voids or air

In the theoretical model shown in figure 9, it is assumed that the shapes of the dots are perfect spherical cap shapes. However, after annealing, some dots have distorted shapes. The distortion of the dots will vary the surface area of the dot. At the same time, it also changes the interfacial area between the dot and the substrate. Consequently, the distortion of the dots will affect its free energy and it may affect the dot transfer ratio. However, it is difficult to determine the effect of distortion of the dots on the dot transfer ratio. Further study is necessary.

4. Conclusion

(i) A new process to fabricate gold nanodot array on a plastic film by transfer technique is proposed in this study. This method obtains high transfer ratio.

(ii) The silicon substrate results higher transfer ratio than the quartz glass substrate. This is attributed to the difference between the surface energy of the substrates.

(iii) The plastic materials show contrary trends of variation of transfer ratio against annealing temperature. Araldite rapid epoxy decreases the transfer ratio while the SpeciFix-20 epoxy

increases transfer ratio when the annealing temperature becomes higher. This is attributed to the difference between the viscosities of the epoxies.

(iv) Dot transfer mechanism is discussed theoretically and compared with the experimental results.

Acknowledgements

FE-SEM observation was carried out at the Center for Advanced Materials Analysis in Tokyo Institute of Technology.

References

[1] Eustis, S., El-Sayed, M. A., Why Gold Nanoparticles Are More Precious than Pretty Gold: Noble Metal Surface Plasmon Resonance and Its Enhancement of the Radiative and Nonradiative Properties of Nanocrystals of Different Shapes. Chem.Soc. Rev. 2006, 35, 209–217.
[2] Pillai S., Green M. A., Plasmonics for photovoltaic applications, Solar Energy Materials & Solar Cells 94 (2010) 1481–1486.
[3] Yguerabide, J., Yguerabide, E. E., Light-Scattering Submicroscopic Particles as Highly Fluorescent Analogs and Their Use as Tracer Labels in Clinical and Biological Applications I. and II. Anal. Biochem. 1998, 262, 137–176.
[4] Min Hu, Carolina Novo, Alison Funston, Haining Wang, Hristina Staleva, Shengli Zou, Paul Mulvaney, Younan Xia and Gregory V. Hartland, Dark-field microscopy studies of single metal nanoparticles: understanding the factors that influence the linewidth of the localized surface plasmon resonance, J. Mater. Chem., 2008,18, 1949-1960.
[5] El-Sayed, I. H., Huang, X., El-Sayed, M. A., Surface Plasmon Resonance Scattering and Absorption of Anti-EGFR Antibody Conjugated Gold Nanoparticles in Cancer Diagnostics: Applications in Oral Cancer. Nano Lett. 2005, 5, 829–834.
[6] Sagle, L. B., Ruvuna, L. K., Ruemmele, J. A., Van Duyne, R. P, Advances in localized surface plasmon resonance spectroscopy biosensing, Nanomedicine (2011) 6(8), 1447–1462.
[7] Haes, A. J., Van Duyne, R. P., A Nanoscale Optical Biosensor: Sensitivity and Selectivity of an Approach Based on the Localized Surface Plasmon Resonance Spectroscopy of Triangular Silver Nanoparticles. J. Am. Chem. Soc. 2002, 124, 10596–10604.
[8] Katherine, A. W., Van Duyne, R. P., Localized Surface Plasmon Resonance Spectroscopy and Sensing, Annual Review of Physical Chemistry, Vol. 58, 2007, 267-297.
[9] Jeffrey, N. A., Hall, W. P., Lyandres, O., Shah, N. C., Jing, Z., Van Duyne, R. P., Biosensing with plasmonic nanosensors, Nature Materials vol. 7, no. 6, pp. 442-453, 2008.
[10] Huang, X., El-Sayed, I. H., Qian, W., El-Sayed, M. A., Cancer Cell Imaging and Photothermal Therapy in the Near-Infrared Region by Using Gold Nanorods. J. Am. Chem. Soc. 2006, 128, 2115–2120.
[11] Huang, X., Jain, P. K, El-Sayed, I. H., El-Sayed, M. A., Gold Nanoparticles: Interesting Optical Properties and Recent Applications in Cancer Diagnostics and Therapy, Nanomedicine 2007, 2, 681–693.
[12] O'Neal, D. P., Hirsch, L. R., Halas, N. J., Payne, J. D., West, J. L. Photo-thermal Tumor Ablation in Mice Using near Infrared-Absorbing Nanoparticles. Cancer Lett. 2004, 209, 171–176.
[13] Maria, L., Maria, M. G., Giuseppe, V. B., Alberto, S., Pio, C., Giovanni, B., Enhanced absorption in Au nanoparticles/a-Si:H/c-Si heterojunction solar cells exploiting Au surface plasmon resonance, Solar Energy Materials & Solar Cells 93 (2009) 1749–1754.
[14] Nakayama, K., Tanabe, K., Atwater, H. A., Plasmonic nanoparticle enhanced light absorption in GaAs solar cells, Applied Physics Letters 93, 121904 (2008).
[15] Wen, L., Xiaodong, W., Yueqiang, L., Zhaoxin, G., Fuhua,Y., Jinmin, L., Surface plasmon enhanced GaAs thin film solar cells, Solar Energy Materials & Solar Cells 95 (2011) 693–698.
[16] Moulin, E., Sukmanowski, J., Schulte, M., Gordijn, A., Royer, F.X., Stiebig, H., Thin-film silicon solar cells with integrated silver nanoparticles, Thin Solid Films 516 (2008) 6813–6817.
[17] Jain, P. K., Lee, K. S., El-Sayed, I. H., El-Sayed, M. A., Calculated Absorption and Scattering Properties of Gold Nanoparticles of Different Size, Shape, and Composition: Applications in Biological Imaging and Biomedicine. J. Phys. Chem. B 2006, 110, 7238–7248.
[18] Kelly, K. L., Coronado, E., Zhao, L. L., Schatz, G. C., The Optical Properties of Metal Nanoparticles: The Influence of Size, Shape, and Dielectric Environment. J. Phys. Chem. B 2003, 107, 668–677.
[19] Chou, S. Y., Krauss, P. R., Renstrom, P. J., Imprint of sub-25 nm vias and trenches in polymers, Appl. Phys. Lett. 67 (1995), 3114.
[20] Yao, C. H., Hsiung, H. Y., Sung, C. K., Influences of process parameters and mold geometry on direct nanoimprint, Microelectronic Engineering 86 (2009) 665–668.
[21] Akahane, T., Huda, M., Tamura, T., Yin, Y., Hosaka, S., Orientation-controlled and long-range-ordered self-assembled nanodot array for ultrahigh-density bit-patterned media, Japanese Journal of Applied Physics 50 (2011) 06GG04.
[22] Sebastian, S., Christopher, K., Jae-Byum, C., Karl, K. B., Sub-10 nm structures on silicon by thermal dewetting of platinum, Nanotechnology 21 (2010) 505301 (7pp).
[23] M. Yoshino, H. Ohsawa, A. Yamanaka, Rapid fabrication of an ordered nano-dot array by the combination of nano-plastic forming and annealing methods, J. Micromech. Microeng. 21 (2011) 125017 (9pp).
[24] Jaccodine, R. J., Surface Energy of Germanium and Silicon, J. Electrochem. Soc. 1963, Volume 110, Issue 6, pp 524-527.
[25] Shchipalov, Y. K., Surface energy of crystalline and vitreous silica, Glass and Ceramics Vol. 57, Nos. 11 – 12, 2000, pp8-11.

Appendix

Assume that the dots are sphere cap shape; contact angle is constant for all dots; volume of metal layer is conserved through the annealing process. Metal evaporation does not occur; and diameters and alignment of nanodots are random. The contact angle θ of the random nanodot array is determined as following equations:

When $0 \le \theta \le \pi/2$

$$f(\theta) = \frac{1}{\sin^3\theta}\left(2 - 3\cos\theta + \cos^3\theta\right) = \frac{24At}{\pi \sum_{i=1}^{N} {D_i}^3} \quad (1)$$

When $\pi/2 \le \theta \le \pi$

$$f(\theta) = \left(2 - 3\cos\theta + \cos^3\theta\right) = \frac{24At}{\pi \sum_{i=1}^{N} {D_i}^3} \quad (2)$$

Where, A is the area of observation. t is initial thickness of the coated metal layer. D_i is diameter of a nanodot. The values of A an D_i are determined from FE-SEM micrograph by a graphic analysis system.